ISTANBUL
UNIVERSITY
CERRAHPASA

An Effective Method for Islanding Detection Based on Variational Mode Decomposition

Solgun Salimi (ID), **Amangaldi Koochaki** (ID)

Electrical Engineering Department, Aliabad Katoul Branch, Islamic Azad University, Aliabad Katoul, Iran

ABSTRACT

The present study presents a new islanding detection method based on variational mode decomposition (VMD). In the method, the VMD transform of the voltage at point of common coupling is calculated, and then based on the decomposed modes, an islanding detection index for distinguishing between islanding and normal conditions will be derived. Pursuing this objective, the measured voltage is decomposed into four modes, and a new islanding detection index will be derived from their energy and their variations. Then, thresholds will be adjusted based on values of proposed index in various conditions on normal and islanding operations. The proposed algorithm decomposes the measured signal into a predetermined number of intrinsic modes around central frequencies; the method is insensitive to the noise and sampling frequency. To validate the method, a distribution network has been simulated in PSCAD/EMTDC, and the algorithm is tested on a variety of islanding and normal circumstances. The results illustrate desired performance of the proposed algorithm for conditions such as motor, nonlinear, and large load switching; as normal condition; and islanding condition with a variety of power mismatches between local load and distributed generation. The results demonstrate the desired performance of the method with respect to both speed and accuracy.

Keywords: Passive islanding detection, Variational mode decomposition, Energy modes, Threshold, Non-detection zone

Introduction

Islanding phenomenon refers to an undesired event in distribution networks consisting of distributed generations (DGs), where the power is cut-off from the main network while DG continues to supply the load. In such a condition, the detached portion of the network, called the island, is possible to not meet the power quality index requirements, such as voltage and frequency. The phenomenon may lead to the destructive effect on the DG, as well as the network equipment. In this respect, the IEEE standard considers a 2-second limit to disconnect DG from the rest of the network when islanding occurs [1]. The islanding detection methods are generally classified into two main groups, local and remote, based on the side in which islanding is detected. Furthermore, the local methods are grouped into two classes as passive and active methods [2, 3]. The passive methods are exclusively based on the measurement of electrical parameters, such as voltage, current, and frequency at the point of common coupling (PCC) [4-6]. On the other hand, in the active methods, a disturbance signal is injected into the PCC so that it facilitates abnormalities detection at the point [7]. In remote islanding detection, a communication infrastructure is required to transfer data from DG to the remote site located on the main power system [2].

Since disturbance signal is not used in the passive methods, there would be no concern about power quality and network security issues. Unfortunately, the methods have non-detection zone (NDZ) in which detection schemes are unable to detect the islanding condition [1]. Technically, NDZs occur when resonant frequency of the local load is matched with the fundamental frequency of the power system [8]. In contrast, active islanding detection algorithms use a disturbance signal providing smaller NDZs; however, this benefit comes at the price of reduction of power quality, as well as installation of appropriate electronic devices.

Corresponding Author:
Amangaldi Koochaki

E-mail:
Koochaki@aliabadiau.ac.ir

Heretofore, a variety of passive methods are introduced for islanding detection. The most practiced methods are under voltage/over voltage (UV/OV) and under frequency/over frequency (UF/OF) procedures. In these methods, voltage and frequency variations caused by unbalanced active and reactive powers are employed for islanding detection [9-11]. Unfortunately, the methods are characterized with large NDZs. More sensitive techniques have been proposed to improve their detection abilities, such as phase jump [12], rate-of-change-of-frequency [13], and rate-of-change-of-reactive-power. These are featured with large detection errors. Different techniques, such as total harmonic distortion [14,15], power spectral density [7], and network harmonic impedance [5], also have wide NDZs. Moreover, advanced spectral analysis and filtering approaches, including those based on wavelet singular entropy [16], pattern recognition [17], data mining [18], and Bayesian classification [19], are proposed. In wavelet transform-based solutions, a number of decomposed levels are found by the trial-and-error method, and extracted features are highly sensitive to noise [1]. They also call for classification trainings using such artificial intelligence (AI) techniques as artificial neural networks and support vector machine, which has high computational complexity. Approaches based on S-transform have been proposed to avoid problems of wavelet-based methods in islanding detection [20-22]. Although these techniques have solved the noise problem in a sense, they still involved high processing needs and usage of AIs to distinguish between islanding and normal conditions.

The main part of the voltage signal contains more illustrative information about the events on the power line. The signal decomposition helps to discriminate between the noise/harmonics and the main signal. In the present study, a new islanding detection algorithm is proposed based on variational mode decomposition (VMD). The algorithm is non-recursive and decomposes the voltage signal into a predetermined number of intrinsic modes around central frequencies. It has only a few variables, does not need to determine the mother wavelet function, and is not sensitive to the noise and sampling frequency. In the present study, VMD is used to decompose the voltage into four modes, and then based on computing the energy of each individual mode, the new islanding index will be obtained.

The structure of the study is as follows. VMD is introduced briefly in section 2. The proposed algorithm is presented in section 3. The performance of the algorithm through computer simulation in PSCAD/EMTDC and MATLAB software is illustrated in section 4. Finally, the conclusion is given in section 5.

VMD transform

VMD transform decomposes a signal into a given number of constitutive intrinsic mode functions (IMFs). It is a non-recursive signal processing method, an upgraded version of Empirical Mode Decomposition (EMD), which eliminates EMD limits, such as sensitivity to noise and sampling frequency [23, 24]. In

the frequency domain, bandwidth of a mode is spread and limited around a central frequency ω_k (Hz). In the time domain, it corresponds to an AM–FM modulated signal as follows:

$$u_k(t) = A_k(t)\cos\emptyset_k(t). \tag{1}$$

Here, the principle of signal decomposition is the compact bandwidth of IMFs, which will be derived using the following optimization problem [25]:

$$min\left\{\sum_k \left\|\partial_t\left[\left(\delta(t)+\frac{j}{\pi t}\right)*u_k(t)\right]exp^{-i\omega_k t}\right\|_2^2\right\} \tag{2}$$

$$s.t. \sum_k u_k = f(t).$$

Where k is the number of modes that main signal f must be composed to, and $\{u_1,\dots,u_k\}=\{u_k\}$ and $\{\omega_1,\dots,\omega_k\}=\{\omega_k\}$ are sets of all modes and central frequencies, respectively. To solve the problem, both quadratic penalty factors and Lagrange multipliers are used to obtain an unconstrained optimization problem as follows:

$$\mathcal{L}(\{u_k\},\{\omega_k\},\lambda) =$$

$$\alpha\sum_k \left\|\partial_t\left[\left(\delta(t)+\frac{j}{\pi t}\right)*u_k(t)\right]exp^{-i\omega_k t}\right\|_2^2 + \left\|f(t)-\sum_k u_k(t)\right\|_2^2 + \langle\lambda(t),f(t)-\sum_k u_k(t)\rangle. \tag{3}$$

Where α is the weighting parameter for constraints. The saddle point of augmented Lagrangian (L) must be found through sequentially iterative suboptimizations called alternative direction method of multipliers (ADMMs) to solve this minimization problem in Equation (2).

The algorithm of ADMM optimization concept for VMD is

Initialize $\{u_k^1\},\{\omega_k^1\},\lambda^1, n\leftarrow 0$

Repeat

$n\leftarrow n+1$

For k=1:K **do**

Update u_k

$$u_k^{n+1}\leftarrow arg_{u_k}min\mathcal{L}(\{u_{i<k}^{n+1}\},\{u_{i\geq k}^n\},\{\omega_i^n\},\lambda^n). \tag{4}$$

End for

For k=1:K **do**

Update ωk

$$\omega_k^{n+1}\leftarrow arg_{\omega_k}min\mathcal{L}(\{u_i^{n+1}\},\{\omega_{i<k}^{n+1}\},\{\omega_{i\geq k}^n\},\lambda^n). \tag{5}$$

End for

Dual ascent

$$\lambda^{n+1}\leftarrow\lambda^n+\tau\left(f-\sum_k u_k^{n+1}\right). \tag{6}$$

Until convergence: $\sum_k\frac{\|u_k^{n+1}-u_k^n\|_2^2}{\|u_k^n\|_2^2}<\epsilon. \tag{7}$

To update u_k, the first suboptimization in Equation (4) must be rewritten as the following minimization problem:

$$u_k^{n+1} = arg_{u_k \in X} min \left\{ \alpha \left\| \partial_t \left[\left(\delta(t) + \frac{j}{\pi t} \right) * u_k(t) \right] exp^{-j\omega_k t} \right\|_2^2 + \left\| f(t) - \sum_i u_i(t) + \frac{\lambda(t)}{2} \right\|_2^2 \right\}. \quad (8)$$

Then, applying Parseval/Plancherel Fourier isometry, variable changes, and Hermitian symmetry of real signal, the frequency spectrum of each individual mode can be obtained without difficulty. Accordingly, the filtered modes then must go through an inverse Fourier transform to obtain the corresponding time domain signals [25].

$$\hat{u}_k^{n+1}(\omega) = \frac{f(\omega) - \sum_{i \neq k} \hat{u}_i(\omega) + \frac{\lambda(\omega)}{2}}{1 + 2\alpha(\omega - \omega_k)^2} \quad (9)$$

To find the central frequencies, the subproblem in Equation (5) must be rewritten as the following minimization problem:

$$\omega_k^{n+1} = arg_{\omega_k} min \left\{ \left\| \partial_t \left[\left(\delta(t) + \frac{j}{\pi t} \right) * u_k(t) \right] exp^{-j\omega_k t} \right\|_2^2 \right\}, \quad (10)$$

which gives:

$$\omega_k^{n+1} = \frac{\int_0^\infty \omega |\hat{u}_k(\omega)|^2 d\omega}{\int_0^\infty |\hat{u}_k(\omega)|^2 d\omega}, \quad (11)$$

which locates each new ω_k at the gravitational center of each mode spectrum [25].

The proposed algorithm for islanding detection based on VMD

VMD is effective tool to extract feature of signals especially non-stationary ones. To derive the proposed algorithm, the given network is first simulated for various operational states existing in both normal and islanding situations. In the normal operation, different operational scenarios, including change in the network demand with respect to entrance/exit of inductive loads, induction motor starting, and nonlinear load, are applied, whereas in the islanding condition, such scenarios with different power mismatches between local load demand and DG generation are practiced.

An important stage in the classification of various phenomena is the choice of appropriate features. The selected features should have minimum computational burden and low dimension. These objectives are followed in the present study. In all scenarios, voltage at PCC is measured and decomposed into four different modes using VMD, and finally, energy of each mode is calculated as:

$$E(k) = \sum_{i=1}^{n} |V(k,n)|^2, \quad (12)$$

where V refers to decomposed modes of voltage (V), k to the kth mode, n to the number of samples, and E is a value in relation with energy (J). Second, a window of limited length, here 24 samples, is moved along the calculated energies (E) to derive the variation rate of each energy window. If present, the difference between steeps of two consecutive windows is called ΔE_k. Then, based on the exhaustive study of various operational conditions, the following islanding detection index is defined as:

$$IslIndx = \frac{\Delta E_1 * \Delta E_3}{E_4 * \Delta E_2}, \quad (13)$$

where ΔE, i, and E_4 are the variation rates of energy of decomposed modes and energy of fourth mode, respectively. An islanding index in the form of Equation (13) gives large thresholds, and therefore, higher reliability. To achieve more accurate and more reliable results, especially in the presence of strong noises and/or higher harmonic distortions, a number of modes can be increased sufficiently. Here, α=2000 and T=0 are assumed for the parameters of VMD, since in this proposed method only the modes whose central frequencies are close to the network operation frequency have considered noise effects substantially resolved. In addition, NDZ is more squeezed into a smaller area. These are the most significant strength points of this proposed algorithm.

The numerical results of the proposed islanding index demonstrate significant differences between islanding and normal
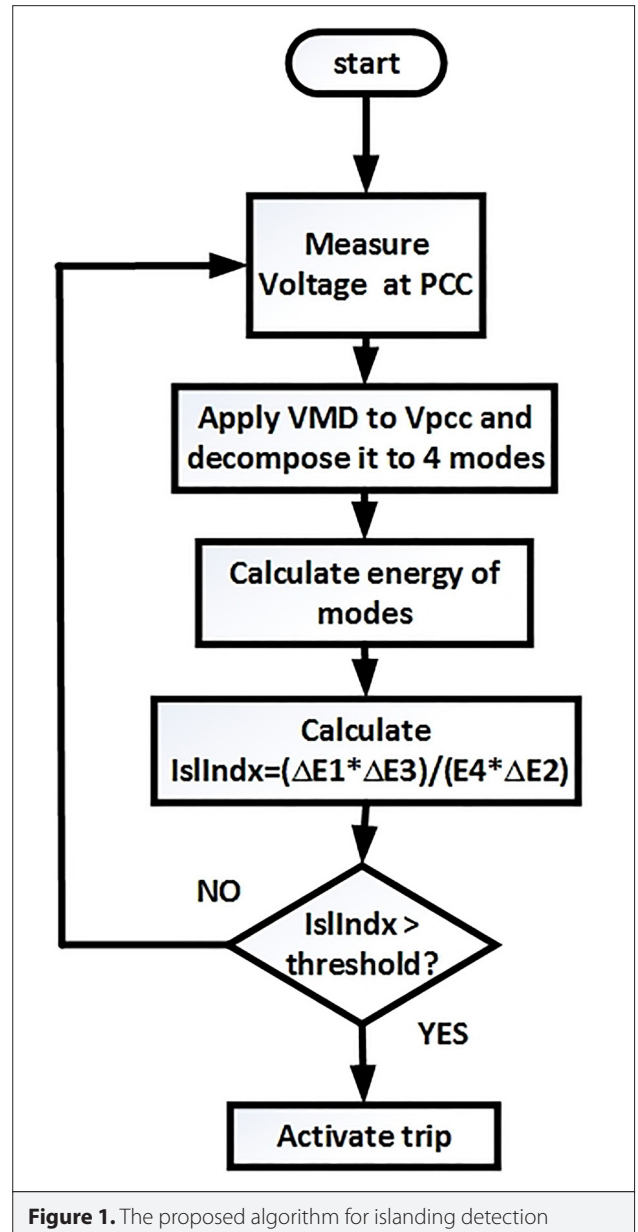

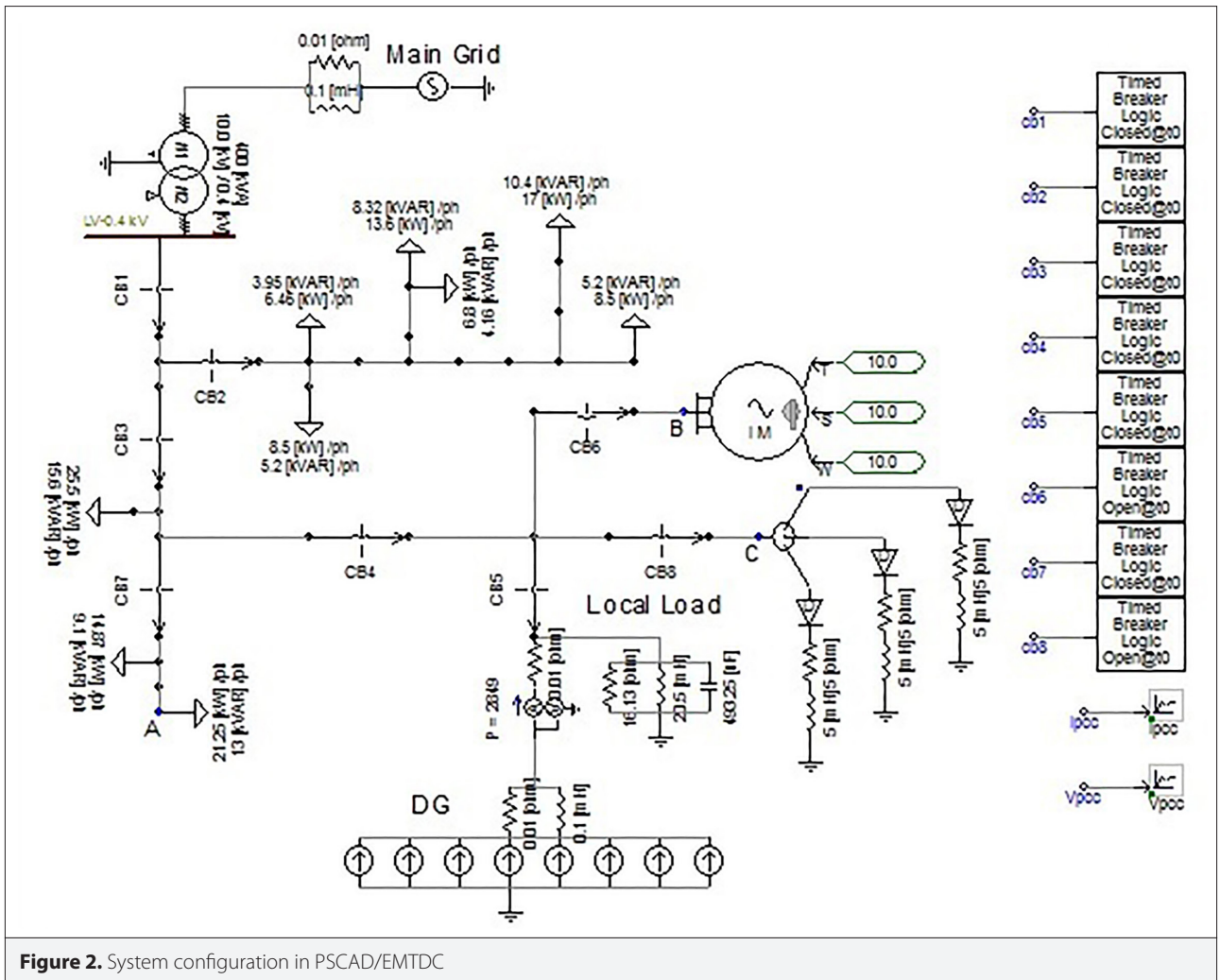**Figure 1.** The proposed algorithm for islanding detection

Figure 2. System configuration in PSCAD/EMTDC

conditions of the network. Thus, it can be used as a practical scale for islanding detection. The differences are meaningful, even for the worst-case scenario where DG's power is completely matched to that of its local load. Considering the worst-case results as a reference, one can adjust thresholds to be so small that the islanding detection is possible, even for the most load balanced states, and so large that no false alarm is produced during the normal operation of the network. Figure 1 illustrates the flowchart of the algorithm. In this figure, ΔE_i and i=1, 2, 3 are the changes of energy for modes 1, 2, 3, and E_4 indicates the energy of the 4th mode.

Simulation results

For the purpose of validity, a low voltage distribution network has been simulated within PSCAD/EMTDC software environments (Figure 2). The main side of the network is a feeder that receives power from a 10/0.4 kV transmission substation and delivers it to a commercial region with a variety of loads. A 3 KW inverter-based DG is connected to a branch of the feeder. Local load is an RLC load with R=16.13 Ω, L=20.5 mH, C=493.25 µF, and Q_f=2.5 (quality factor). System parameters are available in reference [6].

Six scenarios are studied to test the performance of the algorithm. In the first scenario, while the network is in the normal state, CB2 is opened at t=0.6 s, resulting in the reconfiguration and disconnection of a large load; however, the network still continues operation normally. In the second and third scenarios, CB4 and CB5 are opened, respectively, and islanding condition occurs. The second scenario encompasses a large imbalance of power, whereas the third scenario remains nearly in the balance condition. The fourth scenario deals with a 37 kVA induction motor at point B and t=0.4 s, for both adding to and removing from the network. In this case, the network remains at its normal state. In the fifth scenario, the proposed algorithm is tested and verified against nonlinear loads. Finally, in the last scenario, the effect of local load quality factor is investigated.

Normal condition with large load switching

When the system operates under normal condition, by the opening of CB2, a large load is removed from the system and creates a change in voltage and impedance seen from the DG viewpoint. Nonetheless, the algorithm performs correctly and produces no trip signal. Figure 3 and 4 depict the simulation results of this

scenario. Figure 3 shows the main voltage and its decomposed modes, in which there are minor changes at the moment of CB2 opening. Figure 4 shows the energy of the decomposed modes and the calculated index. As can be seen from Figure 4, this situation does not lead to activating a trip. According to the figures, when such a large load as 0.3pu is disconnected from the network (i.e., the worst case of load elimination in the present study), higher values must be selected for the threshold of islanding index.

Islanding condition with large power imbalance

Here, CB4 is opened, and an islanding occurs along with a large power imbalance between DG generation and island demand powers (Figure 5, 6). As it is obvious in Figure 5, there are significant changes in PCC voltage and its decomposed modes at 0.6s (islanding occurrence time), which result in considerable changes in their energies in Figure 6. Figure 6 shows higher

value of calculated index than selected threshold (0.4), which could activate a trip (Figure 6). The results show that the trip signal is 10ms after islanding occurrence. Sensible changes in islanding index are apparent, and thus the algorithm decides properly. Similarly, openings of CB1 and CB3 result in islands and power imbalances and thus easily detectable.

Islanding condition with low power imbalance

In the worst case where CB5 is opened, the DG's generated power is matched exactly to the demand of the islanded area. In this case, UV/OV- and UF/OF-based methods are not able to detect the islanding phenomenon. However, the proposed algorithm is able to detect islanding occurrence. Figure 7 and 8 illustrate the results of simulation for a local load with a 2.5 quality factor. In addition, changes appear to be small in Figure 7, but there are differences that result in more changes in en-
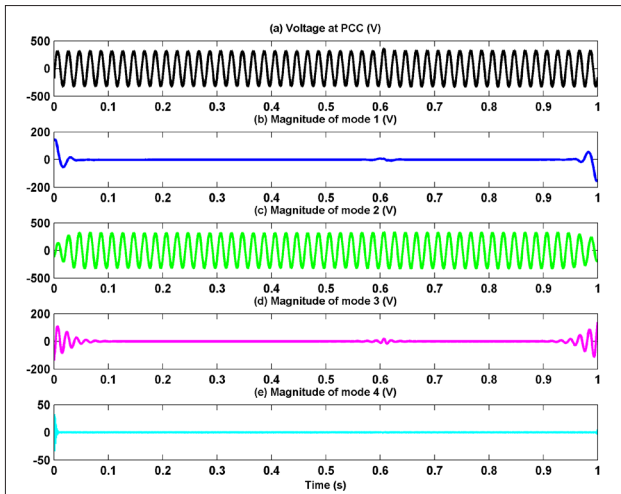

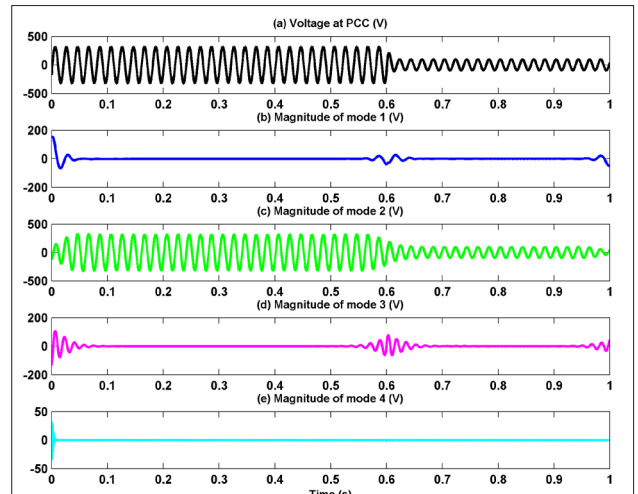**Figure 3.** The voltage at PCC and the decomposed modes for large load switching

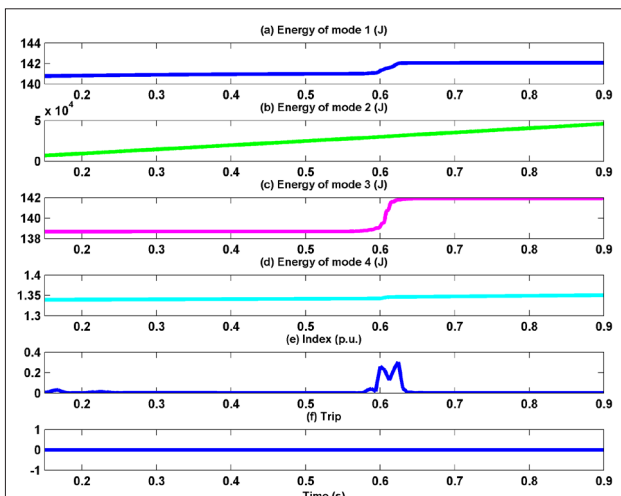**Figure 5.** The voltage at PCC and the decomposed modes for large power imbalance

Figure 4. Change in energies of modes, proposed index, and trip signal for large load switching
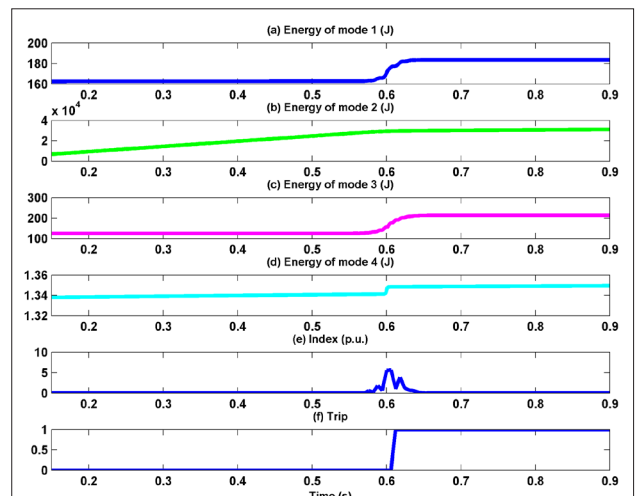

Figure 6. Change in energies of modes, proposed index, and trip signal for large power imbalance

ergies of decomposed modes and produce an effective index (Figure 8). Again, changes in islanding index are sensible, and trip signal is activated in Figure 8. The results show that the algorithm performs successfully in the worst case of islanding.

Normal condition with induction motor starting

Here, a 37kVA induction motor is connected to point B at t=0.4 s. The local load parameters are similar to previous scenarios. Figure 9 shows no meaningful changes in the voltage and decomposed modes. In Figure 10, changes of energies of decomposed modes and the value of islanding index are not considerable. Thus, trip signal is not activated in Figure 10. The results show that the algorithm decision is correct, and no islanding is detected upon the entrance of the induction motor. This scenario is simulated for removing the motor form network. The results show similarly acceptable performance.

Normal condition with nonlinear load switching

In this set-up, a diode nonlinear load is applied to the network at point C and t=0.6 s. Figure 11 and 12 show the corresponding results for this case. The proposed method properly detects no-islanding condition and relatively insensitive to the entrance of the nonlinear load. This scenario is also simulated for the case of the same load exit with similarly acceptable performance.

Effect of the local load quality factor

In the previous scenarios, the quality factor Q_f was assumed to be 2.5. In this section, to analyze the sensitivity of the proposed algorithm to Q_f of local load, the worst-case scenario is repeated to Q_f=3.5. According to Eq. (3) of reference [5], the local load that may lead to worst-case islanding is ($L = \frac{R}{\omega Q_f}, C = \frac{Q_f}{\omega R}$). Thus for R=16.13 Ω and Q_f=3.5, we have L=14.7 mH and C=690.55
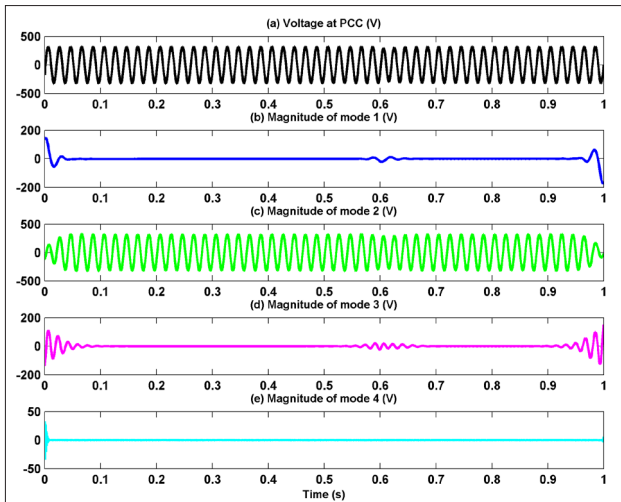

Figure 7. The voltage at PCC and the decomposed modes for low power imbalance
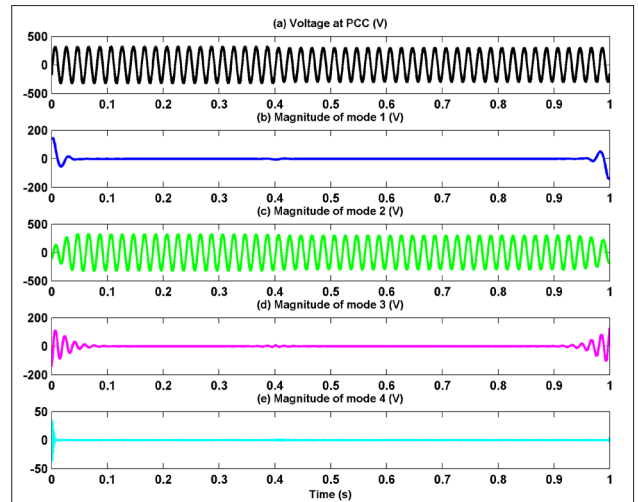

Figure 9. The voltage at PCC and the decomposed modes for induction motor starting
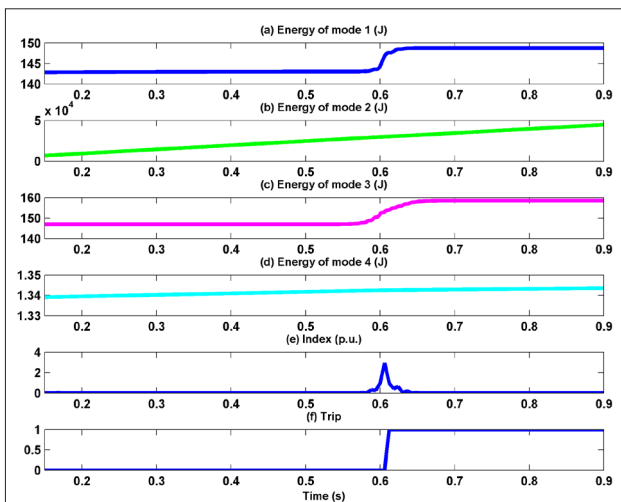

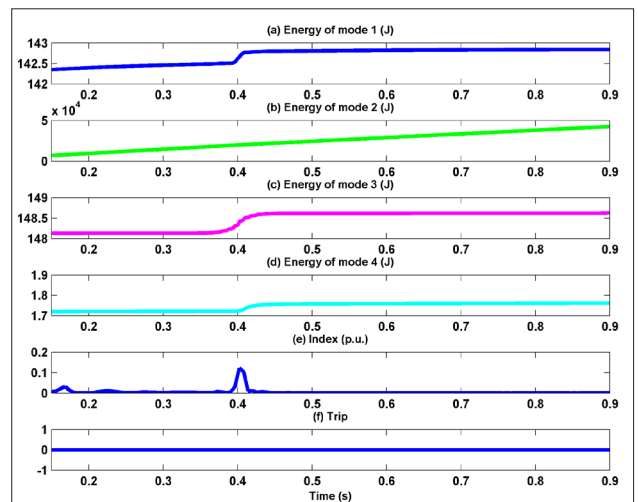**Figure 8.** Change in energies of modes, proposed index, and trip signal for low power imbalance

Figure 10. Change in energies of modes, proposed index, and trip signal for induction motor starting

μF. The simulation results for this case show that the suggested islanding index is relatively insensitive to Q_f, and islanding is positively detected (Figure 13).

More specifically, the index decreases versus increases in Q_f, where for extremely high Q_f, it enters the NDZ regions. To quantify this effect, simulation was replicated for Q_f=1.5, 4, 5. Although the results of simulation for this case display sensitivity of the new islanding index to the defined thresholds and Q_fs, they also illustrate comparable performance of the index versus other similar methods. In case that the threshold is considered to be 0.4, local load and DG active powers are equal, and Q_f=5, this method faces misjudgment. Since the calculated islanding index is 0.35, the algorithm goes into an NDZ state. Therefore, it is decisive to adjust thresholds against worst-case islanding situation and/or worst-case load connection/disconnection in the network's normal operating condition.
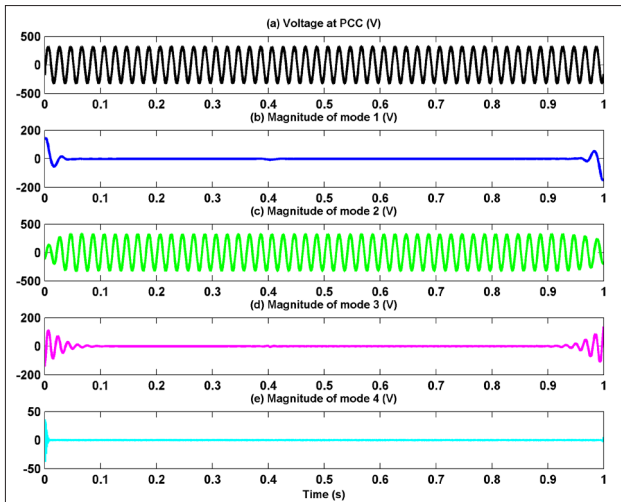
Threshold setting

Threshold setting is an important issue in the passive islanding detection approaches. An inappropriate threshold may lead to NDZ or failing detection zone (FDZ). When powers of load (demanded) and DG (generated) are equal and power factor is one, a remedy to this problem is to assume the worst-case islanding scenarios and consider the minimum value of the index. On the other hand, the most important scenarios to be considered for threshold adjustment are those of connection/disconnection of large load, start-up of induction motors, and nonlinear loads in all of which cases the maximum value of the islanding index is suggested in normal operating conditions. To avoid NDZ and FDZ simultaneously, we must have the following:

$$Max(IslIndx)\ of\ normal < TH < Min(IslIndx)\ of\ islanding. \quad (14)$$

Figure 11. The voltage at PCC and decomposed modes for non-linear load switching
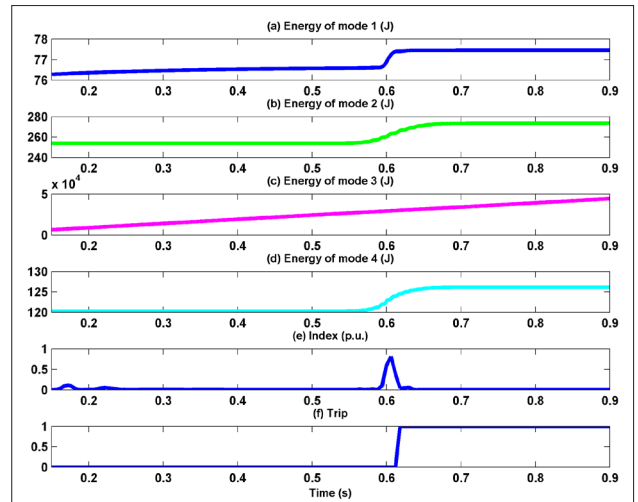
Figure 13. Change in energies of modes, proposed index, and trip signal for Qf=3.5
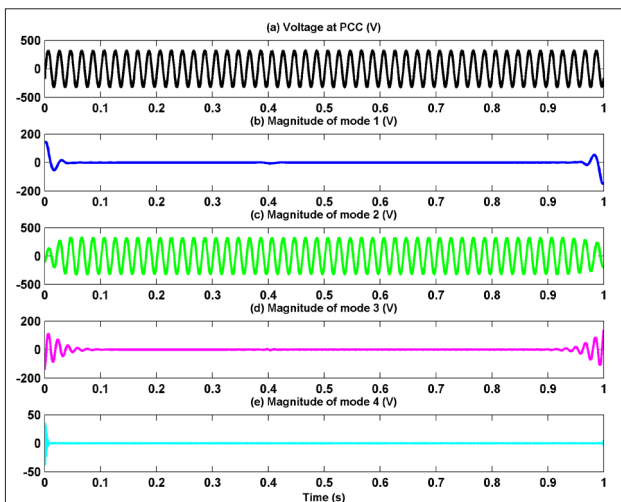

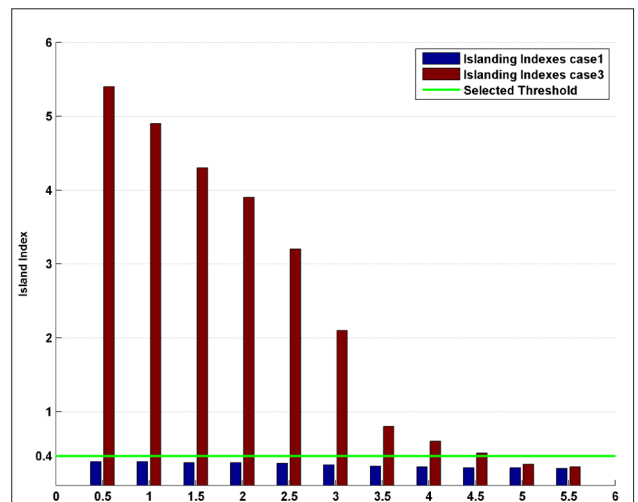**Figure 12.** Change in energies of modes ,proposed index, and trip signal for nonlinear load switching

Figure 14. Threshold setting.

Where TH is the threshold. Figure 14 demonstrates an example for the application of Equation (14) for a range of Q_f values. In this situation, R is assumed to be constant, the local Q_f is variable, and the IslIndx index is calculated according to Equation (14). More clearly, if CB2 is opened for any reason, a large load is eliminated from the network while the whole system continues its normal operation. In such a case, thresholds must be tuned for FDZ avoidance. From another point of view, if CB5 is opened, the worst case of islanding phenomenon occurs. In addition, here, thresholds must be adjusted with respect to NDZ avoidance.

As it is shown in Figure 14, a threshold value equal to 0.4 pu makes islanding detection possible except for $Q_f s > 5$, whereas for all the cases of normal network conditions, the detector remains silent (no islanding). Altogether, it is suggested to adjust thresholds in such a way that they decrease NDZ and avoid FDZ at the same time.

Analysis of noise effect

The existence of noise in power systems is obvious. It causes susceptibility problems for the previous methods, such as those based on wavelet and S-transforms. The proposed islanding detection relies on VMD transform, which is well known for such desired characteristics as high immunity against noise.
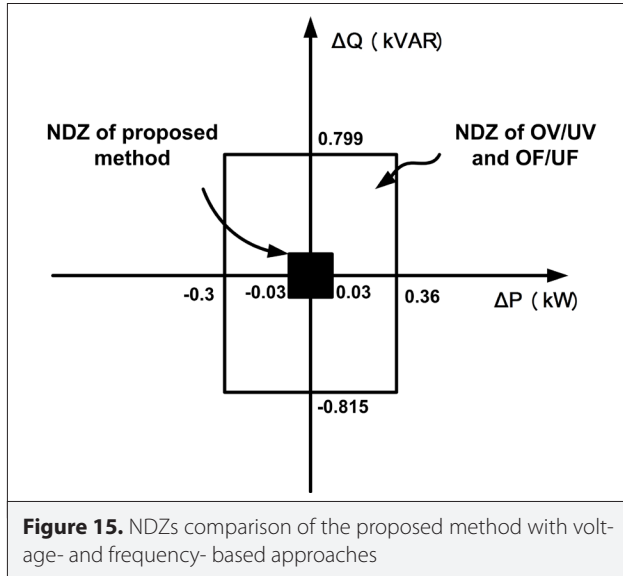
To analyze our algorithm with respect to this feature, the first simulation (normal condition with large load switching) and third simulation scenarios (islanding condition with lower imbalance) were replicated in the presence of noise where signal-to-noise-ratio is assumed to be 20dB, for both islanding and no-islanding situations. The method is decided properly, in both the presence and absence of islanding phenomenon. In addition, the accuracy of the proposed index has been compared with those of other indexes, numerically, as shown in Table 1. The superior accuracy of the new islanding method is self-expressive. Moreover, contrary to the -wavelet transform and fast discrete S- transform based approaches, it is not dependent to the precision of classifications built upon AIs.

NDZ analysis

NDZ is an important parameter for the diagnosis of islanding occurrence. It specifies a zone/zones in which islanding is not detected in the appropriate time. In the present study, the inverter is of constant-current-controlled type. Thus, to determine the power imbalance levels, the following steps are done leading to islanding detection in OV/UV and OF/UF algorithms. For NDZ detection, the level of the active power imbalance (w) is equal to [28]:

$$\Delta P = -3V \times I \times \Delta V, \tag{15}$$

where V and I are the nominal voltage (V) and current (A) of the DG, respectively. According to IEEE 1547-3003 [29] and

Figure 15. NDZs comparison of the proposed method with voltage- and frequency- based approaches

Table 1. Comparison of the proposed islanding method with those of the other methods for SNR=20 dB

Detection time	Average accuracy (%)	Method
0.31 s	97.66	Probabilistic NN [26]
<20 ms	83.63	ST [27]
50 ms	70.6	WT [27]
<20 ms	87.87	FDST+SVM [27]
45 ms	91.5	FDST+BELM [27]
10 ms	98.7	Proposed method

SNR, signal-to-noise-ratio; SVM, support vector machine; NN, neural network; ST, S-transform; WT, wavelet transform; FDST, fast discrete S-transform; BELM, bidirectional extreme learning machine

Table 2. Comparison of the proposed islanding method with some other methods

Principle	Classification	Detection time	NDZ
Frequency	Passive (frequency dependent impedance) [6]	150 ms	Very small
Wavelet	Passive (discrete wavelet transform) [30]	<20 ms	Very small
Frequency	Active (slip mode frequency shift [12]	198 ms	Small
Combination	Passive (rate-of-change-of reactive power and current THD) [14]	60 ms	Not available
Proposed method	Passive (energy index of decomposed voltage)	Approximately 10 ms	Very small

NDZ, non-detection zone; THD, total harmonic distortion

VDE-0126-1-1, if voltage is in the range of 0.88 pu and 1.1 pu, the voltage relays must not take action, i.e., for $\Delta V = -0.12$ and $\Delta V = 0.1$ pu. Accordingly, the active power imbalance levels of the present study (when the nominal output power of DG's inverter is 3 kW) would be 0.36 kW and -0.3 kW. In addition, the level of imbalance in the reactive power after islanding equals that of the local reactive demand (VAR) just before the event [28].

$$\Delta Q = \frac{3V^2}{\omega_n L}\left(1 - \frac{\omega_n^2}{\omega_r^2}\right) \tag{16}$$

Where ω_n and ω_r are frequencies (Hz) of the system and load resonance, respectively. The unbalanced reactive power resulted of the islanding provides rises to a drift in the resonance frequency, so:

$$\omega_r = \omega_n + \Delta\omega, \omega_r = 1\big/\sqrt{LC}. \tag{17}$$

Moreover, the relationship between the frequency and the reactive power deviations becomes:

$$\Delta Q = \frac{3V^2}{\omega_n L}\left(1 - \frac{f_n^2}{(f_n + \Delta f)^2}\right). \tag{18}$$

According to reference [29], the acceptable ranges of frequency deviations are within 49.7 and 50.3 Hz, i.e., $\Delta f = \pm 0.3$ Hz. For the given case study, these are, in order, equivalent to -0.815 and 0.799 kVARs.

Figure 15 compares the NDZs of the proposed method with those of OV/UV and OF/UF for a DG characterized by nominal power and constant-current control mode. For validation purposes, we simulated power imbalances ranging from -10% to 12% of the nominal power, as a result of islanding occurrence, with 0.01 precision totaled to 23 steps in increasing order. It is worth mentioning that both the voltage- and frequency-based approaches have been easily capable of islanding detection. The time duration for an event to be diagnosed as either islanding or normal was assumed to be 1 s. It can be seen clearly from Figure 15 that the NDZ of the suggested method is significantly smaller than those of the other ones. Performance of the proposed method is compared with the other ones as shown in Table 2. The comparison shows that the proposed VMD-based method has better detection time than the other ones; in addition, the NDZ of the method is very small.

Conclusion

A new method for islanding detection based on VMD was proposed. At first, the measured voltage signal was decomposed into its principal modes using VMD. Next, energies of individual modes were calculated as the bases for discrimination between islanding and normal conditions. The algorithm was then applied to various scenarios, including islanding presence, no islanding with different levels of power imbalance, and diversities of load quality factors using simulations. The results of the simulation illustrated acceptable performance of the proposed algorithm with respect to both accuracy and speed, even for the worst-case islanding.

References

1. H. Vahedi, G. B. Gharehpetian, M. Karrari, "Application of duffing oscillators for passive islanding detection of inverter-based distributed generation units", IEEE Trans. on Power Delivery, vol. 27, no. 4, pp. 1973-1983, Oct. 2012. [CrossRef]
2. D. Velasco, C.L. Trujillo, G. Garcerá, E. Figueres, "Review of anti-islanding techniques in distributed generators", Renewable and Sustainable Energy Reviews, vol. 14, no. 6, pp. 1608-1614, 2010. [CrossRef]
3. V. Task, "Evaluation of islanding detection methods for photovoltaic utility interactive power systems", in International energy agency implementing agreement on photovoltaic power systems, Tech. Rep.IEA-PVPS T5-09, March 2002.
4. F. De Mango, M. Liserre, A. Dell'Aquila, A. Pigazo, "Overview of anti-islanding algorithms for PV systems. Part I: passive methods", 12th International Power Electronics and Motion Control Conf., Portoroz, 2006, pp. 1878-1883. [CrossRef]
5. N. Liu, C. P. Diduch, L. Chang, J. Su, "A reference impedance-based passive islanding detection method for inverter-based distributed generation system", IEEE Journal of Emerging and Selected Topics in Power Electronics, vol.3, no.4, pp. 1205-1217, 2015. [CrossRef]
6. N. Liu, A. Aljankawey, C. Diduch, L. Chang, J. Su, "Passive islanding detection approach based on tracking the frequency-dependent impedance change", IEEE Trans. on Power Delivery, vol. 30, no. 6, pp. 2570-2580, Dec. 2015. [CrossRef]
7. J. Yin, C. P. Diduch, L. Chang, "Islanding detection using proportional power spectral density", IEEE Trans. on Power Delivery, vol. 23, no. 2, pp. 776-784, April 2008. [CrossRef]
8. A. Yafaoui, B. Wu, S. Kouro, "Improved active frequency drift anti-islanding detection method for grid connected photovoltaic systems", IEEE Trans. on Power Electronics, vol. 27, no. 5, pp. 2367-2375, May 2012. [CrossRef]
9. A. Ghaderi, M. Kalantar, A. Esmaeilian, "A novel islanding detection method for constant current inverter based distributed generations", 2011 10th International Conference on Environment and Electrical Engineering, Rome, 2011, pp. 1-4. [CrossRef]
10. H. H. Zeineldin, J. L. Kirtley, "Performance of the OVP/UVP and OFP/UFP method with voltage and frequency dependent loads", IEEE Trans. on Power Delivery, vol. 24, no. 2, pp. 772-778, April 2009. [CrossRef]
11. Z. Ye, A. Kolwalkar, Y. Zhang, P. Du, R. Walling, "Evaluation of anti-islanding schemes based on nondetection zone concept", IEEE Trans. on Power Electronics, vol. 19, no. 5, pp. 1171-1176, Sept. 2004. [CrossRef]
12. B. Singam, L. Y. Hui, "Assessing SMS and PJD schemes of anti-islanding with varying quality factor", IEEE International Power and Energy Conf., Putra Jaya, 2006, pp. 196-201. [CrossRef]
13. J. C. M. Vieira, W. Freitas, Z. Huang, W. Xu, A. Morelato, "Formulas for predicting the dynamic performance of ROCOF relays for embedded generation applications", IEE Proceedings - Generation, Transmission and Distribution, vol. 153, no. 4, pp. 399-406, 13 July 2006. [CrossRef]
14. A. Danandeh, H. Seyedi, E. Babaei, "Islanding detection using combined algorithm based on rate of change of reactive power and current THD techniques", Asia-Pacific Power and Energy Engineering Conference, Shanghai, 2012, pp. 1-4. [CrossRef]

15. S. Jang, K. H. Kim, "An islanding detection method for distributed generations using voltage unbalance and total harmonic distortion of current", IEEE Trans. on Power Delivery, vol. 19, no. 2, pp. 745-752, April 2004. [CrossRef]

16. A. Samui, S. R. Samantaray, "Wavelet singular entropy-based islanding detection in distributed generation", IEEE Trans. on Power Delivery, vol. 28, no. 1, pp. 411-418, Jan. 2013. [CrossRef]

17. N. W. A. Lidula, A. D. Rajapakse, "A pattern recognition approach for detecting power islands using transient signals-part I: design and implementation", IEEE Trans. on Power Delivery, vol. 25, no. 4, pp. 3070-3077, Oct. 2010. [CrossRef]

18. K. El-Arroudi, G. Joos, I. Kamwa, D. T. McGillis, "Intelligent-based approach to islanding detection in distributed generation", IEEE Trans. on Power Delivery, vol. 22, no. 2, pp. 828-835, April 2007. [CrossRef]

19. W. K. A. Najy, H. H. Zeineldin, A. H. K. Alaboudy, W. L. Woon, "A Bayesian passive islanding detection method for inverter-based distributed generation using ESPRIT", IEEE Trans. on Power Delivery, vol. 26, no. 4, pp. 2687-2696, Oct. 2011. [CrossRef]

20. S. Alshareef, S. Talwar, W. G. Morsi, "A new approach based on wavelet design and machine learning for islanding detection of distributed generation", IEEE Trans. on Smart Grid, vol. 5, no. 4, pp. 1575-1583, July 2014. [CrossRef]

21. P. K. Ray, N. Kishor, S. R. Mohanty, "S-transform based islanding detection in grid-connected distributed generation based power system", IEEE International Energy Conference, Manama, 2010, pp. 612-617. [CrossRef]

22. M. Mishra, P. K. Rout, "Time-frequency analysis based approach to islanding detection in micro-grid system", Int. Rev. Electr. Eng. (IREE), vol.11, no.1, pp.116-129, 2016. [CrossRef]

23. F. Babaei-Roudi, A. A. Abdoos, "Detection of internal fault from external fault and inrush current in power transformers based on combination of VMD and ELM", Computational Intelligence in Electrical Engineering, vol. 9, no. 1,pp. 65-77, 2018.

24. P. D. Achlerkar, S. R. Samantaray, M. S. Manikandan, "Detection of voltage variation events using variational mode decomposition", IEEE PES Asia-Pacific Power and Energy Engineering Conference (APPEEC), Bangalore, 2017, pp. 1-6. [CrossRef]

25. K. Dragomiretskiy, D. Zosso, "Variational mode decomposition", IEEE Transactions on Signal Processing, vol. 62, no. 3, pp. 531-544, Feb.1, 2014. [CrossRef]

26. F. Hashemi, M. Mohammadi, "Islanding detection approach with negligible non-detection zone based on feature extraction discrete wavelet transform and artificial neural network", Int. Trans. Electr. Energ. Syst., vol. 26, pp. 2172-2192, 2016. [CrossRef]

27. M. Mishra, PK. Rout, "Fast discrete s-transform and extreme learning machine based approach to islanding detection in grid-connected distributed generation," Energy Syst, pp. 1-33, 2016. [CrossRef]

28. H. H. Zeineldin, E. F. El-Saadany, M. M. A. Salama, "Impact of DG interface control on islanding detection and non detection zones," IEEE Transactions on Power Delivery, vol. 21, no. 3, pp. 1515-1523, July 2006. [CrossRef]

29. IEEE Standard for Interconnecting Distributed Resources into Electric Power Systems, IEEE standard 1547TM, June 2003.

30. A. Pigazo, M. Liserre, R. A. Mastromauro, V. M. Moreno, A. Dell'Aquila, "Wavelet-based islanding detection in grid-connected PV systems," IEEE Transactions on Industrial Electronics, vol. 56, no. 11, pp. 4445-4455, Nov. 2009. [CrossRef]

Solgun Salimi was born in 1981; received the B.Sc in electrical engineering from the Faculty of Electrical Engineering, k. N. Toosi University, Iran, in 2003; she received M.Sc from Aliabad Katoul Branch of Islamic Azad University, Iran, in 2017. Her research interests are power system analysis, islanding detection algorithms.

Amangaldi Koochaki was born in 1981; received the B.Sc in electrical engineering from the Faculty of Electrical Engineering, University of Tehran, Iran, in 2003; he received M.Sc and Ph.D from Amirkabir University of Technology, Iran, in 2003 and 2010 respectively. Now he is assistant professor in Aliabad Katoul branch of Islamic Azad University, Iran. His research interests are power system analysis, relay coordination and renewable energies.